Proposal for a new FINUDA data taking

FINUDA Collaboration

February 15, 2008

Abstract

In this report we present a proposal for a new FINUDA data taking, soon after the end of SIDDHARTA run, explaining its motivations in the light of the results achieved so far by FINUDA and of the International scenario. Our purpose is to collect on selected nuclei a statistics one order of magnitude larger than in the past, to fix significatively the physics topics currenlty under investigation.

Contents

Chapter 1

Introduction

The idea of carrying out a Hypernuclear Physics program at the (e^+, e^-) DAΦNE Φ-Factory was put forward in 1991 [1]. A Collaboration (FINUDA-FIsica NUcleare a DAΦNE) comprising 6 Institutions with about 40 physicists was quite rapidly settled and less than two years later a Proposal [2] and a Technical Design Report [3] were submitted to LNFSC. The experiment was approved in 1995. The national Committee for Nuclear Physics (Gr.III) supported strongly the experiment since the beginning, securing the necessary budget without applying heavy cuts and/or restrictions on the requests. Up to now, the total budget provided to FINUDA is about 13 Millions of Euros for durables and investments, about 8 Millions of Euros for consumables and travel expenses. It must be recalled that the original schedule of DAΦNE foresaw a start-up of the commissioning of the machine in 1995, with the goal of reaching a peak luminosity of 5×10^{32} cm^{-2}s^{-1}. Even by allowing quite a long time for the commissioning of a new machine aiming to an ambitious luminosity goal, the financing profile and the related schedule of preparation of the different parts of the detector (magnet, sub-detectors, infrastructures) were such that FINUDA was ready around 1999 and able to carry out a unique program in Hypernuclear Physics and other K induced nuclear reactions even at an initial luminosity of 10^{32} cm^{-2}s^{-1}.
Before recalling briefly the main items of the original FINUDA Physics program and the proposed extension, it is worthwhile to stress some points. The production reaction of Hypernuclei is

$$K^- +^A \mathrm{Z} \rightarrow^A_\Lambda \mathrm{Z} + \pi^- \tag{1.1}$$

with K^- stopped in nuclear targets. The main advantage of carrying out measurements of observables using the (1.1) reaction induced by the low energy (16 MeV) K^- from Φ-decay is that the K^- can be stopped in very thin (typically 200 mg/cm^2) targets. This feature brings many advantages (small corrections for the energy loss in the target of the produced charged particles, including deuterons and also heavier nuclear fragments, little dispersion angles due to multiple Coulomb scattering,...). In other words very clean experimental data may be obtained by FINUDA.

Two counterpart disadvantages must be faced. The first one is that, even at the "dreamt" luminosity of 5×10^{32} cm^{-2}s^{-1}, the number of K^- (about 1000

s^{-1}) was lower than what could be delivered at existing (1995) machines (AGS at BNL, 12 GeV PS at KEK). This figure is very low if compared with that expected at the J-PARC facility in Tokai (Japan) that will start its operations next year. This limitation of DAΦNE was counterbalanced by the design and construction of a magnetic spectrometer (FINUDA) with a cylindrical geometry featuring a solid angle larger than 2π for the detection of π^- from reaction (1.1) and other reaction products sr. The structure of the spectrometer was such that an energy resolution of about 1 MeV on the produced Hypernuclear states was obtained, better than the one reached with forward spectrometers, which covered a solid angle typically of 100 msr. In these experiments the Hypernuclear states were produced by the reaction (1.1) in flight (typically at 800 MeV/c) or with the (π^+, K^+) reaction at about 1.2 GeV/c. In conclusion the product ($\phi_{MT} \times \Delta\Omega$), where ϕ_{MT} is the flux of the mesons (π^- or K^+) tagging the formation of a well defined Hypernuclear state, and $\Delta\Omega$ the detection solid angle, was larger for the (FINUDA + DAΦNE) complex, at the design luminosity of 5×10^{32} cm^{-2}s^{-1}.

The same spectrometer could be used for the precise determination of the momentum of other charged particles emitted in coincidence with the π^- from reaction (1.1). Therefore, thanks to its design and advanced performances, FINUDA could collect at the same time all the available information also on other different physics topics. From the same data bulk, by applying different selection criteria, the momentum resolution could be optimized at the expense of the statistics, by accepting only "clean" tracks defined by four points in the tracking detectors and a good enough χ^2. On the contrary, when statistics was the primary goal in studies in which several particles had to be detected in coincidence, the criteria for "clean" tracks could be relaxed, accepting also, for instance, backward tracks or lower resolution tracks reconstructed by three points only. Fig. 1.1 (taken from Ref. [4]) shows an example of the data collected for the K^{-12}C in the 2003-2004 run. Fig. 1.1a) shows the momentum spectrum of π^- from all the ^{12}C targets, obtained with the selection criteria optimized for hypernuclear spectroscopy. The relative momentum resolution is 0.6 % fwhm. The dashed curve represents the contributions of π^- coming from two-nucleon K^- absorption reaction

$$K^- + (np) \to \Sigma^- + p \tag{1.2}$$

followed by the Σ^- decay in flight:

$$\Sigma^- \to n\pi^- \tag{1.3}$$

Fig. 1.1b) shows the momentum spectrum obtained by relaxing the selection criteria on the quality of the tracks; the resolution worsens by a factor of 2, but the statistics increases by a factor of 6.

FINUDA was the first experiment in Hypernuclear Physics to use an advanced vertex detector using Si-microstrips. Among the many tasks performed by this detector, it allowed the identification and separation of the primary vertices from the reactions (1.1) and (1.2) from those from Hyperon weak decays (like (1.3)).

Unfortunately, due to the time needed for the commissioning of the machine and to the scheduling of the experiments, 5 years passed before FINUDA could

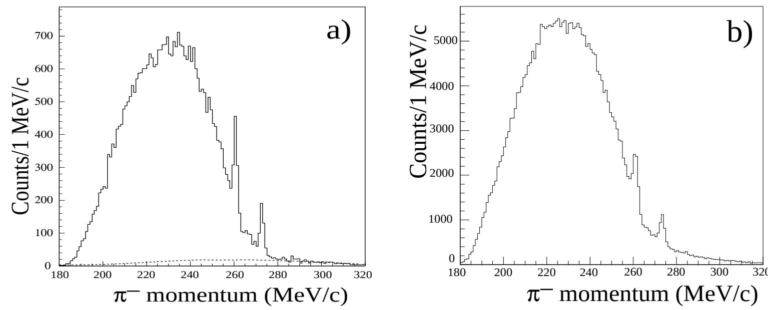

Figure 1.1: a) Momentum spectrum of π^- from ^{12}C targets, obtained with the selection criteria optimized for hypernuclear spectroscopy with good energy resolution. The dashed line represents the contribution from K^- absorption by two nucleons. b) Momentum spectrum of π^- from ^{12}C targets obtained using more relaxed selection criteria in track fitting, inclusing backwards tracks. From Ref. [4].

start the first (engineering+data) data taking (October 2003). A total of 250 pb^{-1} (190 for physics) were delivered for a first look at the physics items that could still be competitive. Infact, during the five years of delay, some of the measurements foreseen in the original FINUDA proposal were carried out at other Laboratories (KEK, BNL), mostly in the Spectroscopy and Weak Decays sectors.

For the first survey, targets made of ^{6}Li, ^{7}Li, ^{12}C, ^{27}Al and ^{51}V were used. No measurements on medium A targets were performed before. The measurements at FINUDA showed that reaction (1.1) has a reasonable capture rate for p-shell nuclei only, and the following analyses were focused mostly on light Hypernuclei. In spite of the delay, original and very interesting results were obtained on Spectroscopy ([5, 6]), Non Mesonic Weak Decays [4], and search for neutron-rich light Hypernuclei [7]. However the unique combination of the clean K^- source (DAΦNE) and the very transparent and complete detector optimized for the study of the interactions of Kaons in thin nuclear targets (FINUDA) allowed new measurements to be performed, not foreseen in the original proposal, such as a study of the ^{7}Li(K$^+$, K^0) reaction close to threshold [8] and topics related to the possible existence of Deeply Bound Kaon States (DBKS). The interest in such an item was triggered by a theoretical suggestion by Akaishi and Yamazaki [9] about possible aggregates of a few nucleons strongly bound by a K^- and with a narrow width. These systems should have a density even ten times larger than the usual nuclear matter one, with a potential great impact on the comprehension of the origin and structure of the neutron stars. With FINUDA a clean reconstruction of the free Λ particle by means of its invariant mass can be achieved, as shown in Fig. 1.2.

The Λ momentum can be measured down to 100 MeV/c, as shown in Fig. 1.3). The lower limit is imposed by the threshold on proton momenta, which must exceed 100 MeV/c for the particle to come out of the targets.

We stress that neither existing nor proposed detectors are able to measure lower p_Λ momenta. Furthermore we want to draw the attention to the two

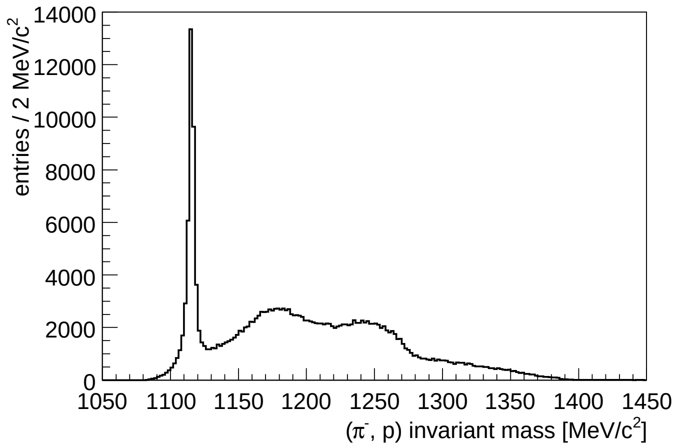

Figure 1.2: $(\pi^- p)$ invariant mass, obtained with long tracks and secondary vertex selection. The Λ peak is clearly identified.

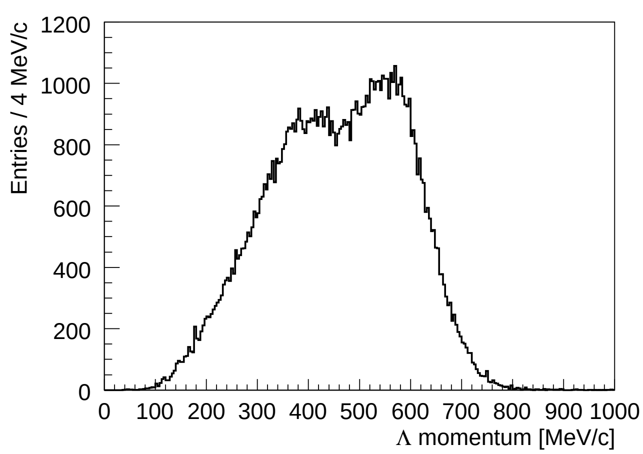

Figure 1.3: Λ momentum as reconstruced by FINUDA.

bump structure in Fig. 1.3. The second bump at $p_\Lambda \simeq 590$ MeV$/c$ derives from K^-_{stop} interaction on correlated nucleons, and this is the region of paramount importance for a thorough understanding of the existence and nature of DBKS. This unique experimental feature allowed the invariant mass method to be applied for the first time in the search for DBKS. The first candidate was found for the $(K^- pp)S$ system ([10], top cited paper). An experiment aiming to confirm the existence of such a state was approved with top priority at the J-PARC machine complex [11] and will run next year. Further analyses on the DBKS subject were performed in order to clarify the importance of the quasi-free ab-

sorption processes on correlated nucleon pairs [12], and studying the invariant mass of the the (Λd) system [13]. We shall return on this point later.
With the experience and physics information acquired in the first run, we installed for a second long run (962 pb^{-1}, December 2006–June 2007) a new target assembly, composed of ^{6}Li (2×), ^{7}Li (2×), ^{9}Be (2×), ^{13}C and ^{16}O. The main physics goals were to obtain more statistics 1) on the (Λp) and (Λd) correlated pairs produced in the absorption of K^- on many nucleons, 2) on the nucleon spectra from Non Mesonic Weak Decay (NMWD), 3) on the search for the $^{6}_{\Lambda}$H and $^{7}_{\Lambda}$H neutron-rich Hypernuclei, and 4) on several other items like Hypernuclear Spectroscopy and (K^+, K^0) Charge Exchange reactions on nuclei close to threshold. After the necessary calibrations of the detector, the analysis of the new data sample has just started and is in good progress [14]. Very interesting signals have been observed since the very beginning. The most interesting ones are the appearance of a very clean (Λt) correlation, following the absorption of a K^- by nuclei, and the measurement of the proton spectra from NMWD down to the lowest energy ever [15], which seems to indicate the importance of the two-nucleon induced NMWD. We shall come back on these points in the following Sections.

The signals we have observed are very interesting and clean, but they suffer from a limited statistics. For these reasons we feel useful to concentrate our efforts on a new run with a total integrated luminosity of 3 fb^{-1} dedicated to the study of the interactions of stopped K^- with two kinds of nuclear targets only : ^{6}Li (4 targets) and ^{12}C (2 targets). In the following we will describe these motivations in detail.

With the new crab waist interaction region, the K^- in the antiboost region will not have enough energy to pass through the first layer of Si micro-strip detectors and they will stop in them. It could therefore be possible to get information on the hypernuclear spectroscopy and NMWD from $^{28}_{\Lambda}$Si.

Finally we outline the absolute need of FINUDA to start the run as quickly as possible (this year, beginning of next year at most). The time window in which FINUDA is still competitive and unique will be closed by the start up of J-PARC, foreseen for the second half of 2009.

We do not deem worth running later.

Chapter 2

Hypernuclear Physics

2.1 Non Mesonic Weak Decays

The importance of the Non Mesonic Weak Decay of Hypernuclei was recognized since the early days of Hypernuclear Physics [16]. It is the most spectacular example of Nuclear Medium modification (defined by variation of the intrinsic properties of an elementary particle when embedded in a nucleus), even though such a feature was scarcely emphasized. Furthermore it is the “easiest” way to get information of the four baryon weak process $\Lambda N \rightarrow NN$, with possble hints also on the ΛNN interaction. In spite of these very appealing features, the process of NMWD of Hypernuclei has been scarcely studied on the experimental side for a few decades, essentially due to experimental difficulties. Indeed it was not only mandatory to identify Hypernuclei in their ground states but also to detect and measure the energy of the emitted protons and neutrons.
The first complete measurement was performed in 1991 by Szymanski et al. [17] at BNL using the (K^-,π^-) reaction at 800 MeV/c to produce and tag ${}^{5}_{\Lambda}$He and ${}^{12}_{\Lambda}$C hypernuclei, with limited statistics. Proton spectra emitted from ${}^{12}_{\Lambda}$C formed through the (π^+,K^+) reaction with π^+ of 1.05 GeV/c at KEK were measured by Noumi et al. [18]. However, the largest amount of data on NMWD was produced by the SKS Collaboration at KEK, from 2000 to 2005. The (π^+,K^+) reaction was used to produce copiously Hypernuclei in their ground state [19, 20, 21, 22, 23, 24].

The main emphasis on the recent measurements performed with the SKS spectrometer was put on the experimental determination of the ratio of the neutron induced NMWD width Γ_n to the proton induced one Γ_p. There has been a long standing "puzzle" concerning the Γ_n/Γ_p ratio. The values reported by the former experiments, even though with large errors, were close to or larger than 1, whereas the simple one-pion exchange model with ΔI=1/2 rule foresaw values one order of magnitude lower. In Ref. [23] a value of about 0.5 was measured in agreement with recent theoretical values obtained with improved one-meson exchange models [25] and direct-quark exchange mechanism [26]. Quite recent review articles on the subject are due to Outa [27] for the experimental aspects and to Alberico and Garbarino [28] for the theoretical approaches.

It must be noticed that, if on one side the most important questions on NMWD were qualitatively solved, discrepancies still exist between theory and experiments. As outlined by Bauer et al. [29] the experimental proton spectra are incompatible with those evaluated from theoretical models. For this reason we have done an analysis of the proton spectra from NMWD of ${}^{5}_{\Lambda}$He, ${}^{7}_{\Lambda}$Li and ${}^{12}_{\Lambda}$C taking advantage of the unique features of the FINUDA spectrometer, *i.e.* the trasparency, the use of thin targets and the measurement of the proton energies by magnetic analysis. The thin targets permit to lower the threshold down to 15 MeV, the lowest energy ever. The result of this analysis have been accepted for publication by Nucl.Phys. A [30].

Let us recall that proton spectra had been measured in the past by few experiments, and not really very cleanly. Proton spectra from NMWD of ${}^{5}_{\Lambda}$He and ${}^{12}_{\Lambda}$C were already studied experimentally [17, 18, 21, 22] and theoretically [25, 28, 29, 32]. For ${}^{7}_{\Lambda}$Li there are neither measurements nor theoretical calculations, in spite it is the best known Hypernucleus from the spectroscopic point of view [31]. The proton spectra from NMWD of ${}^{5}_{\Lambda}$He, ${}^{7}_{\Lambda}$Li and ${}^{12}_{\Lambda}$C from FINUDA are shown by fig.2.1(a,b,c). The spectra show a similar shape, *i.e.* a peak around 80 MeV, corresponding to about a half the Q-value for the free $\Lambda p \to np$ weak reaction, with a low energy rise, due to the final state interactions (FSI) and/or to two nucleon induced weak decays [28, 29, 32].

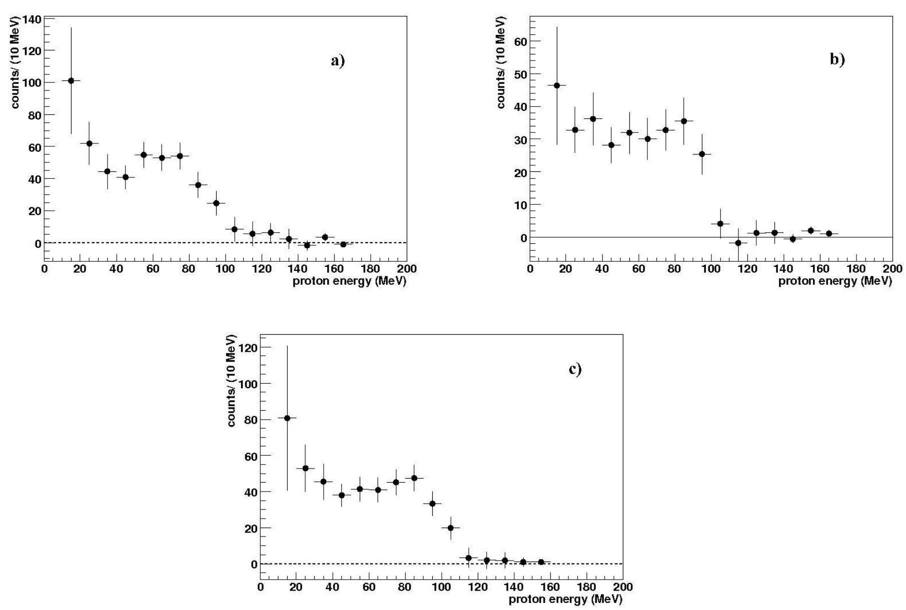

Figure 2.1: Proton energy spectrum after the background subtraction from NMWD of a)${}^{5}_{\Lambda}$He, b) ${}^{7}_{\Lambda}$Li and c)${}^{12}_{\Lambda}$C.

Fig.2.2a) shows the comparison of our spectrum for ${}^{5}_{\Lambda}$He with the one by Okada et al.[21]. The two spectra were normalized beyond 35 MeV (the proton energy threshold of [21]).

Fig.2.2b) shows the comparison of our spectrum with the theoretical one calculated by Garbarino et al.[32]. The two spectra were normalized beyond 15 MeV (our proton energy threshold). Statistical tests indicate that there is

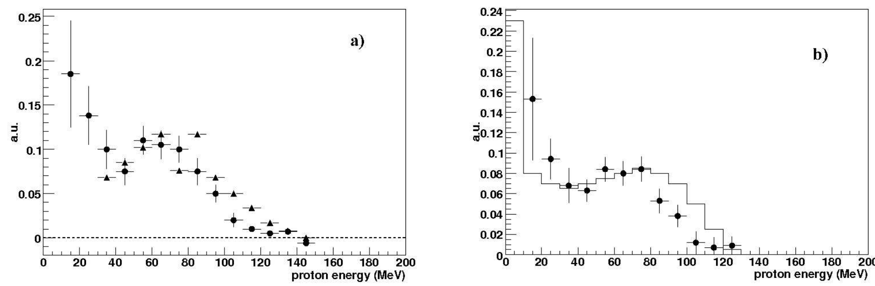

Figure 2.2: a)dots: FINUDA proton spectrum from proton–induced NMWD for ${}^{5}_{\Lambda}$He; triangles: result achieved for the ${}^{5}_{\Lambda}$He at the KEK experiments; the two spectra are normalized to areas beyond 35 MeV. b) Dots: FINUDA experimental proton spectra of ${}^{5}_{\Lambda}$He; continous histogram: theoretical calculation for the proton energy spectrum of ${}^{5}_{\Lambda}$He performed with the addition of the FSI contribution. The two spectra are normalized beyond 15 MeV.

a disagreement between the two experiments and with the theory, even though not so severe.

The situation for ${}^{12}_{\Lambda}$C is completely different. Fig 2.3a) shows the comparison of our spectrum with that by Okada et al.[21]: the two spectra were normalized beyond 35 MeV.

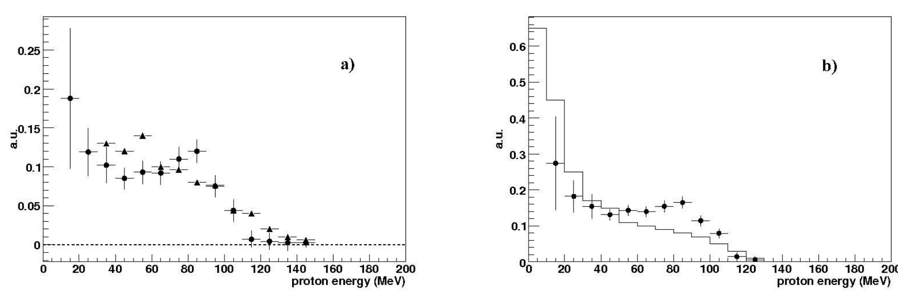

Figure 2.3: Comparison between the proton spectra from NMWD of ${}^{12}_{\Lambda}$C measured by a) FINUDA (dots) and Okada et al.[21] (triangles) normalized beyond 35 MeV; b) comparison between the FINUDA spectrum (dots) and the theoretical calculation performed by Garbarino et al. [32] (histogram) normalized beyond 15 MeV.

Fig 2.3b) shows the comparison of our spectrum with the theoretical one calculated by Garbarino et al. [32]. The two spectra were normalized beyond 15 MeV. Statistical tests on histogram consistency suggest a strong disagreement between the two experiments and with the theory.

Concerning the discrepancy between the two sets of experimental data, we may remark that in Ref. [21] the proton energy was measured by a combination of time-of-flight and total energy deposit measurements. The energy loss inside the thick targets was corrected event-by-event. The energy resolution became poorer in the high energy region, especially above 100 MeV, with the consequence that the spectra could be strongly distorted. On the contrary with FINUDA the proton momenta are measured by means of a magnetic analysis, with an excellent resolution (2% FWHM) and no distortion at all on the spectra is expected, in particular in the high energy region. Our spectrum is the genuinely undistorted one, even though with a limited statistics.

The spectra for ${}^{5}_{\Lambda}$He, ${}^{7}_{\Lambda}$Li and ${}^{12}_{\Lambda}$C look quite similar, in spite of the large mass number difference of these nuclei. If the low energy rises were predominantly due to FSI effects, one should naturally expect the broad peak structure at 80 MeV (coming from clean $\Lambda p \to np$ weak processes broadened by the Fermi motion of nucleons) be smeared out for the heavier nuclei.

Another effect that could be the origin of the low energy rise is a large contribution of the two-nucleon induced weak process $\Lambda np \to nnp$ [28, 32]. If the weak decay Q-value (160 MeV) is shared by three nucleons, a low energy rise may exist even for the very light s-shell hypernuclei. Our data seem to agree with the hypothesis of a substantial contribution of the two-nucleon induced NMWD. Indeed, Bhang et al.[33] recently suggested a contribution of the two-nucleon induced weak decay process as large as 40% of the total NMWD width for ${}^{12}_{\Lambda}$C. However, in order to strengthen this conclusion, there is an urgent need for more data on more medium-A nuclei with much more statistics.

FINUDA is the best detector to give an answer to this important question in the near future. With the proposed choice of targets, we will obtain an increase in statistics of a factor at least 10 for ${}^{12}_{\Lambda}$C, at least 6 for ${}^{5}_{\Lambda}$He. A well grounded conclusion about the importance of the two-nucleon induced weak decay could be at hand.

A comparison with the theoretical calculations would strongly benefit from reduced errors. Last but not least we recall that ${}^{5}_{\Lambda}$He and ${}^{12}_{\Lambda}$C are the only hypernuclei for which detailed theoretical calculations exist and can be implemented quite easily for the comparison with new data [34]. For these reasons we propose to study again ^{12}C with a $\times 10$ statistics.

2.2 Neutron Rich Hypernuclei Search

2.2.1 Physics Motivations

The primary motivation for the proposed search is the possible observation of neutron rich hypernuclear systems with an high N/Z ratio. The most exciting issue is to verify the existence of the heavy hyperhydrogens (N/Z $\geq$ 5). Their observation can provide information on the "glue-like" role of the Λ. In general we know that Λ-hypernuclei are more bound than ordinary nuclei because of the of extra binding energy supplied by the Λ hyperon. Furthermore, the hyperhydrogens could offer the chance to study the Baryon-Baryon interaction in low density nuclear systems. They may also clarify the role of the three body forces, which is enhanced by the Λ-Σ coupling [35].
Narrow resonances of hydrogen isotopes ^{5}H and ^{7}H have been observed recently [36]. Thus the ${}^{6}_{\Lambda}$H and ${}^{8}_{\Lambda}$H hypernuclei might be stable thanks to the well know "glue-like" role of the Λ [37]. The case of the ^{6}H resonance is not well known and understood yet, since there are a lot of discrepancies in old and new

measurements [38]. Therefore we can expect ${}^{7}_{\Lambda}$H to be bound if the ^{6}H ground state energy is below 3 MeV, since it prevents the strong decay ${}^{7}_{\Lambda}$H$\rightarrow{}^{4}{}_{\Lambda}$H+3$n$. Moreover the ^{6}H ground state energy must have a binding energy less than 1 MeV to prevent the decay ${}^{7}_{\Lambda}$H$\rightarrow{}^{6}{}_{\Lambda}$H + n [39]. Furthermore the comparison of ${}^{6}_{\Lambda}$H data with ${}^{7}_{\Lambda}$He data (^{7}Li$(e, e'K^{+})^{7}_{\Lambda}$He reaction will be studied soon at TJNAF [40]), could shed light on a limit of the tree body model (core + n + n). In fact the so called "coherent Λ-Σ coupling effect" (tree body force) should play a major role in the ${}^{6}_{\Lambda}$H systems [41]. From the Astrophysics point of view the deeper knowledge of all these mechanisms is fundamental to understand the State Equation of the high density matter like that of Neutron Stars [42]. The physics impact of heavy hyperhydrogens has motivated scientists to propose experiments in several Labs: Dubna [43], at GSI and FAIR [44], and at J-PARC [45]. The advantage of the mesonic induced reactions (K^{-}, π^{+}) at LNF (FINUDA) and (π^{+}, K^{-}) at J-Parc, over the heavy-ion induced production, is the possibility to observe these states as resonance peaks, which are narrower than for ^{5}H [39]. Furthermore the production rate may be not so small compared to other neutron rich hypernuclei (order of about $10^{-7}K^{-}_{stop}$). For instance, the production of heavy hyperhydrogens through the two step charge-exchange mechanism:

$$K^{-} + p \rightarrow \Lambda + \pi^{0}; \quad \pi^{0} + p \rightarrow n + \pi^{+} \tag{2.1}$$

implies the transitions $1s_{1/2}(p) \rightarrow 1s_{1/2}(\Lambda)$ and $1p_{1/2}(p) \rightarrow 1p_{1/2}(n)$ without change of the quantum numbers, which is usually a favorable situation [39].

2.2.2 Analysis: State of the Art

For the first time, FINUDA studied the ${}^{6}_{\Lambda}$H and ${}^{7}_{\Lambda}$H production using 2003-2004 data. An upper limit of $(2.5 \pm 0.4(stat)^{+0.4}_{-0.1}(syst)) \times 10^{-5}/K^{-}_{stop}$ and $(4.5 \pm 0.9(stat)^{+0.4}_{-0.1}(syst)) \times 10^{-5}/K^{-}_{stop}$ was measured for ${}^{6}_{\Lambda}$H and ${}^{7}_{\Lambda}$H by using the (K^{-},π^{+}) reaction [46]. Fig. 2.4 shows the π^{+} momentum distribution corresponding to the region of ${}^{6}{}_{\Lambda}$H (left) and ${}^{7}{}_{\Lambda}$H (right) formation. The shaded regions of Fig. 2.4 are the regions of interest (ROI), which are centered at the π^{+} momentum value corresponding to the predicted hyperhydrogen B_{Λ}. The ROI widths have been set to $\pm 2\sigma_{p}$, where σ_{p} is the standard deviation of the peak momentum resolution $\sim 0.9\%$ (FWHM).

The analysis of the 2006-2007 data taking is still in progress, and here we report the present state of the art. We select pions against proton or heavier particles using the dE/dx information from OSIM modules, both drift chamber layers and TOF information.This selectively removes the proton contamination in the π^{+} inclusive spectra. Moreover we select well fitted tracks coming from a stopped K^{-}, in order to achieve a resolution on positive tracks of about 0.9% FWHM, as in Ref. [46]. Figure 2.5 shows the π^{+} spectra from ^{6}Li and ^{7}Li targets. The curve is the fitted background, which takes into account the two background reactions:

$$\begin{aligned} K^{-} + p \rightarrow \quad & \Sigma^{+} \quad + \quad \pi^{-} \\ & \hookrightarrow \quad n + \pi^{+} \qquad (\sim 130 < p_{\pi^{+}} <\sim 250 \text{ MeV}/c) \end{aligned} \tag{2.2}$$

$$\begin{aligned} K^{-} + pp \rightarrow \quad & \Sigma^{+} \quad + \quad n \\ & \hookrightarrow \quad n + \pi^{+} \qquad (\sim 100 < p_{\pi^{+}} <\sim 320 \text{ MeV}/c). \end{aligned} \tag{2.3}$$

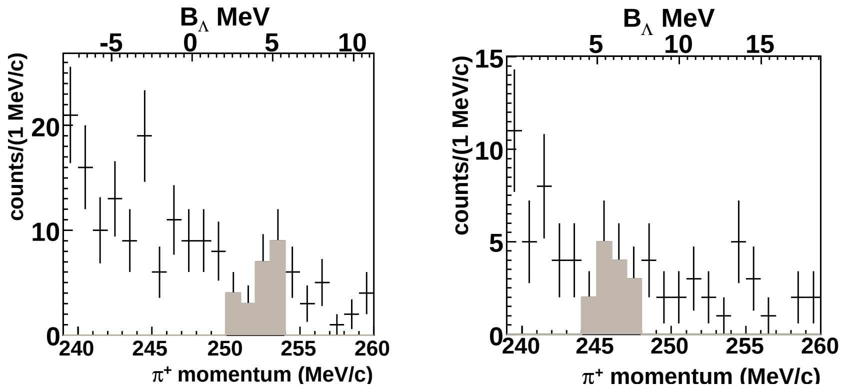

Figure 2.4: π^+ momentum spectra in the region interesting for the search of ${}^6_\Lambda$H and ${}^7_\Lambda$H from ^{6}Li (left) and ^{7}Li (right) targets. Data are from the 2003-2004 run.

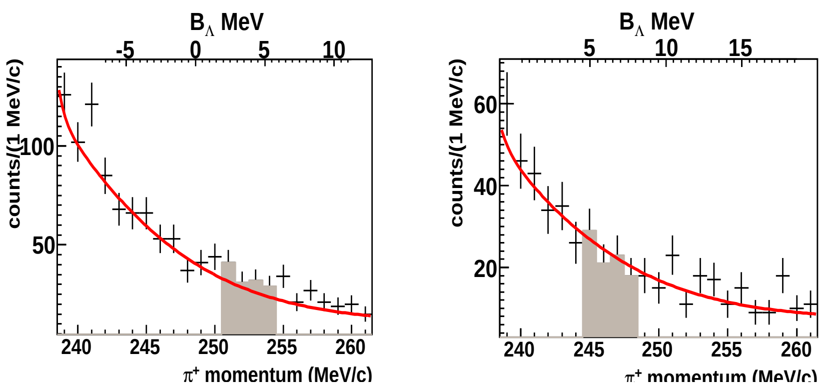

Figure 2.5: π^+ momentum spectra in the region of interest for the search of ${}^6_\Lambda$H and ${}^7_\Lambda$ from ^{6}Li (left) and ^{7}Li (right) targets, 2006-2007 data taking.

As can be seen from figure 2.5 we get ~ 6 times more statistics in the ROIs, but no evidence of signal appears. The Upper Limit for the production rate of ${}^6_\Lambda$H and ${}^7_\Lambda$H is improved of a factor ~ 6, as expected.

In order to improve the signal to background ratio of the possible ${}^6_\Lambda$H and ${}^7_\Lambda$H production, we search for their mesonic decay, since the mesonic decays of the hyperhydrogens are not suppressed as in the case of heavier hypernuclei. In order to increase the statistics we require only fitted tracks for π^- and we release the quality selection on π^+ tracks. Fig. 2.6 shows the π^+ spectra for the events in which a further coincidence with a low momentum π^- (*i.e.* $60 < p_{\pi^-} < 160$ MeV$/c$) is required. The coincidence requirement eliminates the physical background coming from the $K^-\ 2N \to \Sigma^+ n$ reaction (2.3), while survives the physical background from the $\Sigma^+\pi^-$ reaction since these pions have momenta as low as $\sim 100 < p_{\pi^-} < \sim 170$. Finally, the requested coincidence reduces also the possible heavy hyperhydrogens signal rate, when it decays with a Non-Mesonic Weak Decay with two neutrons in the final state. Looking at the Figure, now a possible hyperhydrogen signal ${}^{6}_{\Lambda}$H arises in the ^{6}Li target but its significance is less than 2 σ.

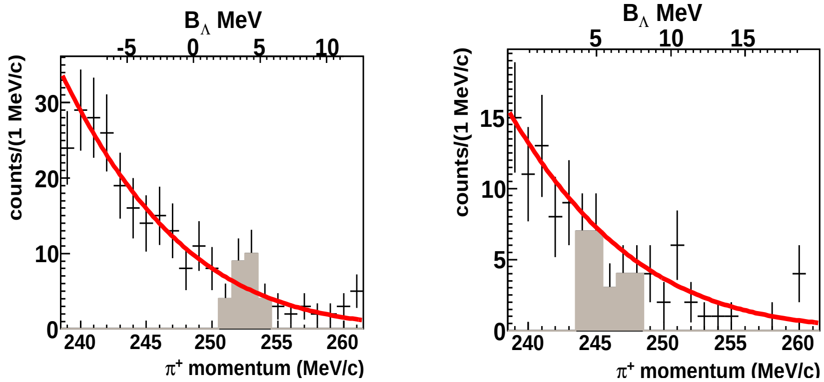

Figure 2.6: π^+ spectra in coincidence with π^- of low momentum ($60 < p_{\pi^-} < 160$ MeV/c), from ^{6}Li (left) and ^{7}Li (right) targets, 2006-2007 data taking

With a total integrated luminosity of 3 fb^{-1} and 4 targets of ^{6}Li we can collect $\sim$ 6 times more statistics in the ROIs. This will increase the statistical significance of the "hint" in the ${}^{6}_{\Lambda}$H region up to 3.5 σ.

2.3 Hypernuclear Spectroscopy

The energy spectrum measured for ${}^{12}_{\Lambda}$C by FINUDA with the data taken in 2003-2004, expressed in Λ binding energy ($-B_\Lambda$) units, is shown in Fig.2.7 [5].

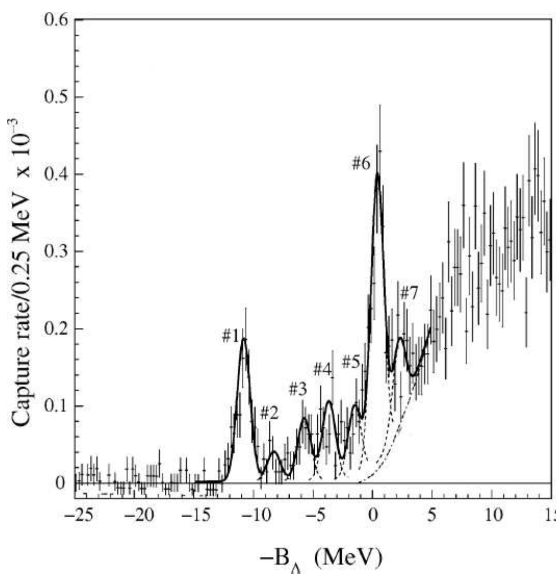

Figure 2.7: FINUDA published results [5] for ${}^{12}_{\Lambda}$C.

The quality criteria applied to select the prompt π^- from the hypernuclear formation are the following: 1) extrapolation of the π^- tracks and stopping vertices of the K^- inside the target volumes; 2) only forward emitted π^-, which cross a minimum amount of materials; 3) well fitted tracks. The spectra due to the physical background affecting the region where hypernuclear levels are present, reactions 1.2 and 1.3, were subtracted using Monte Carlo simulations. Several excited states are observed [5], Fig.2.7, in between the two prominent peaks labelled as #1 and #6, corresponding to the ground state and the p_Λ excited level. Such structures were already reported, with a lower resolution (1.45 MeV) than the FINUDA one (1.08 MeV), in Ref. [47], measured with a different formation reaction with respect to FINUDA: (K^+, π^+). The second and third levels, $J^P=1^-_2$ and 1^-_3, are naturally interpreted as the core-excited states as the $1s^\Lambda$ coupled to the excited levels of the ^{11}C core: $^{11}C(1/2^-_1$; 2.00 MeV) and $^{11}C(3/2^-_2$; 4.80 MeV). Small level shifts from the original core levels can be ascribed to the effects of spin-dependent ΛN interactions. It is also suggested that a possible mixing between Σ and Λ may play a non-negligible effect on these energy shifts. It is believed that recent hypernuclear gamma-ray measurements have determined various spin-dependent ΛN interaction terms such as spin-spin, tensor, symmetric spin-orbit, and antisymmetric spin-orbit terms in p-shell Λ hypernuclei. However, there still exists several specific energy levels which cannot be understood in this framework. The next generation spectroscopic studies with high precision are strongly awaited. In the mean time, high statistics data taken with the existing facilities will be important to confirm the findings and to understand the nature of the spin-dependent interactions.

Very recently, an experiment at TJNAF measured the hypernuclear excitation energy spectrum for the mirror hypernucleus $^{12}_{\Lambda}$B [48]. In this case, too, the used reaction, $(e, e'K^+)$, is different from the FINUDA one, while the resolution is better: 0.67 MeV. These results are shown in Fig.2.8. The similarity of the two spectra is striking: a series of peaks appears as well between the promiment ones, *i.e.* the fundamental (at 0 excitation energy) and the one at an excitation energy of about 11 MeV. All peaks in the two experiments have very similar excitation energies, even if with different populations; only one, present in FINUDA, is absent in the spectrum of TJNAF: this should not be a surprise considering that the hypernucleus formation processes are different and that the formed systems are mirror hypernuclei.

The results of the two experiments for the found peaks are summarized in Table 2.3, in which also the FINUDA results are expressed in excitation energy units for the sake of comparison.

The comparison of the mirror hypernuclei $^{12}_{\Lambda}$C produced by the stopped (K^-, π^-) reaction at FINUDA and $^{12}_{\Lambda}$B by the $(e, e'K^+)$ reaction at TJNAF is interesting, because states with different parities are excited. Another interesting subject are the excited states with the excitation energies in the $(7 \div 11)$ MeV region. Experimentally, a few excited states in this high excitation energy region were observed in the (π^+, K^+) reaction by SKS, $(e, e'K^+)$ reaction at TJNAF, and stopped (K^-, π^-) reaction at FINUDA. However, it is very difficult to interpret them as simple core-excited states, because of their high excitation energy and the excited intensities. It was suggested that, for the positive parity states of $^{12}_{\Lambda}$C in this high excitation region, not only the configuration of $[s^4p^7]_- \otimes 1p^\Lambda$ but also the $([s^4p^6(sd)^1]_+ + [s^3p^8]_+) \otimes 1s^\Lambda$ configurations should

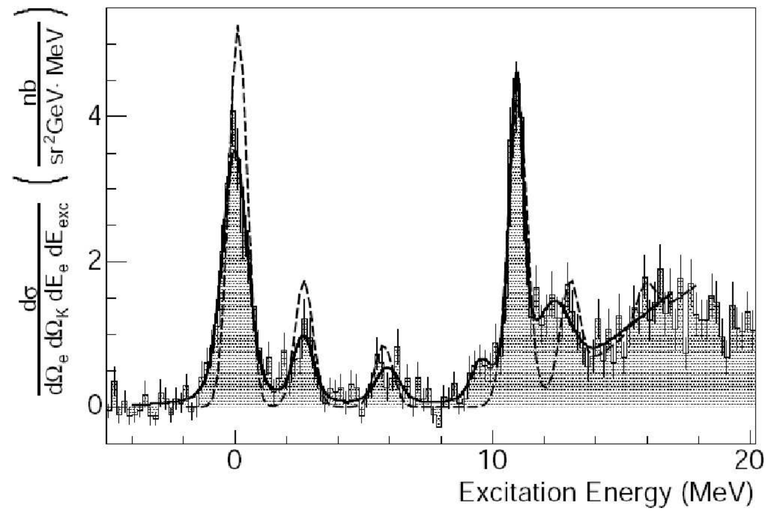

Figure 2.8: TJNAF results for ${}^{12}_{\Lambda}$B [48].

peak #	FINUDA Exc.Energy (MeV)	FINUDA FWHM (MeV)	TJNAF Exc.Energy (MeV)	TJNAF FWHM (MeV)
1	0.00 ± 0.06	1.08 ± 0.19	0.00 ± 0.03	1.15 ± 0.18
2	2.50 ± 0.20	"	2.65 ± 0.10	0.95 ± 0.43
3	5.00 ± 0.10	"	5.92 ± 0.13	1.13 ± 0.29
4	7.10 ± 0.10	"		
5	9.30 ± 0.20	"	9.54 ± 0.16	0.93 ± 0.46
6	11.20 ± 0.07	"	10.93 ± 0.03	0.67 ± 0.15
7	13.0 ± 0.20	"	12.36 ± 0.13	1.58 ± 0.29

Table 2.1: Comparison of FINUDA and TJNAF results on the mirror hypernuclei ${}^{12}_{\Lambda}$C and ${}^{12}_{\Lambda}$B.

be taken into account. Such an extended model calculation with inter-shell couplings was done by T. Motoba [49]. A detailed comparison in this energy region between high resolution data and theoretical calculations will reveal the role of inter-shell couplings for the first time.

The need of a significantly larger statistics clearly emerges in order to confirm all the structures, in particular the less populated ones. On its account, with an integrated luminosity of 3 fb^{-1} and two Carbon targets, FINUDA will provide a tenfold increase of the statistics in the spectrum of fig.2.7.

The upgraded configuration of DAΦNE to reach higher luminosities uses a crossing angle between the e^- and e^+ beams twice as large than in the past: 50 mrad instead of 25 mrad. As a consequence, the created ϕ mesons will have a boost twice as large than in the previous FINUDA data taking. The effect of this experimental situation will greatly affect the two target slots in the full anti-boost side (the maximum/minimum boost-antiboost effect occurs in the horizontal plane). We remind that in FINUDA the K^-, before reaching the targets which are sandwiched between two layers of Silicon microstrips, must cross the beam pipe, the scintillators of the inner tof detector (tofino) and the inner layer of Si microstrips (ISIM). In case of the two target slots most affected by the boost geometry, the K^-'s will mainly stop inside ISIM, and very few will cross it. We can therefore consider the ISIM modules themselves as ^{28}Si targets (at $\sim 92\%$).

^{28}Si is an interesting example of medium heavy nucleus, whose hypernuclear levels and non mesonic weak decays can now be studied. In order to see what we could get from ^{28}Si, even if with a (known) low statistics, we examined the data taken in the previous FINUDA runs, trying to extract the π^- spectrum from K^-'s stopped in ISIM to see its gross features. Of course, also in the past, the two ISIM modules in the full anti-boost side were the most suitable ones for K^- stopping, even if they were mainly transparent, as it should have been. The π^- momentum spectrum deriving from the few K^-'s stopping in the the two anti-boost ISIM modules, from both our data takings, is shown in Fig.2.9: the vertical lines indicate the expected positions of $^{28}_{\Lambda}$Si hypernucleus levels.

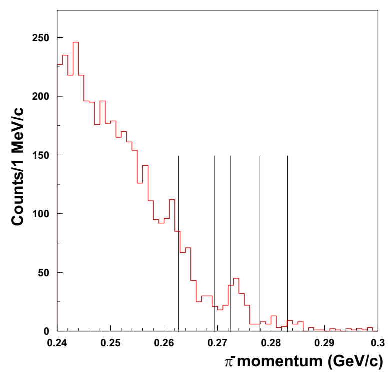

Figure 2.9: π^- inclusive momentum spectrum originating from the two ISIM modules in the anti-boost side, extracted from 2003-2004 and 2006-2007 data.

Looking at the spectra of Fig. 2.9, it should be kept in mind that, to increase the statistics, both forward and backward tracks had to be summed up. Moreover, even for the forward emission (*best tracks*), the track quality is degraded due to the π^- crossing the mounted targets: an unusual, not foreseen situation in FINUDA. In spite of the limited statistics and the unfavoured set-up, some structures clearly emerge, albeit not precisely as expected for the above mentioned reasons, showing that FINUDA has the capability to look at hypernuclear formation by stopped K^- in the ^{28}Si of ISIM modules.

With 3 fb^{-1} of integrated luminosity, we should expect a statistics about 8 times larger with respect to the data shown in Fig.2.9, permitting the usual selection of forward tracks for the study of hypernuclear spectroscopy, in a much cleaner configuration.

Chapter 3

Multinucleon K^- absorption

While the π^- absorption processes in nuclei had been extensively studied in the past decades [50], the absorption of K^-'s by many nucleons (correlated or not) with the emission of baryons is still a rather poorly known process. This study is extremely relevant since the same final states can be populated by K^--nuclear aggregates.

The few existing data on these reactions were collected by old bubble chamber experiments [51, 52] and were mainly focused on the determination of the production rates of final states with pions. In ^{4}He, the branching ratio of non-pionic final states was estimated to be $(16.4 \pm 2.6)\%/K^-_{stop}$, to which the most important contribution was played by the $\Lambda(\Sigma^0)(pnn)$ channel [51]. In Carbon, the multinucleonic branching fraction, per stopped K^-, was reported to be 0.20, and on Neon 0.23 [52] indicating that most probably the K^- absorption takes place at the nuclear surface, and somehow saturates for $A > 4$. It was also believed [53] that the absorption of K^- giving two-body non-mesonic final states was a suppressed reaction.

The absorption reactions have a sizeable overlap with the non-mesonic decay mode of strange multibaryons, which were searched for recently, as the final state particles are the same. Following the theoretical expectations by Akaishi-Yamazaki [9], who are in support of the existence of K^--nuclear aggregates, the K^- and the nucleons should be so tightly bound as to exclude their mesonic decay. From this point of view, disentangling whether a Hyperon-Nucleon (or Nucleus) pair comes from the non-mesonic decay of a strange-nuclear aggregate, or from an absorption reaction on many nucleons is a challenge, which can be solved only by increasing the number of experimental observables. Without a thorough knowledge of the K^- absorption mechanisms it is rather hard to give a final word on the existence of K^--nuclear bound states. With the data collected in the first FINUDA run studies of correlations between a Hyperon and nucleons or light nuclei (deuterons, tritons) were performed. Several results are still preliminary but some indications emerge about the occurrence of absorption processes on more than one nucleon, and of other exclusive reactions which have not such a simple explanation.

In the following we will review the main outcomes from FINUDA analyses in the study of the K^- absorption effects on nuclei which could fake the identification of a genuine Deeply Bound Kaon-Nuclear System (DBKS), pointing out how a new 3 fb^{-1} data taking with the chosen target assembly surely helps to improve our understanding of the experimental data so far collected. The increase of statistics with a 3 fb^{-1} data taking will be decisive for the study of (Λt) (or possibly heavier nuclear fragments) correlations; for the other correlations the increase of statistics must be understood as a useful by-product of the main FINUDA research topics.

We also remark that ^{6}Li is the lightest solid material that can be used as a target in FINUDA. From pion absorption studies [54] it was pointed out that the ^{6}Li nucleus can be understood as a sort of nuclear molecule, composed by a $\alpha + d$ cluster rather loosely bound. It is therefore the most suitable nucleus (besides ^{4}He and ^{3}He, for which, however, the purity is a critical factor) to study K^- absorption effects, both on $2N$, $3N$ and $4N$, as well as with the nucleus as a whole. The small number of nucleons that are involved in the K^- interaction keeps the number of possible final states small, and it allows most of the times to perform a complete kinematic analysis, which is not always possible in heavier nuclear systems. Furthermore, ^{6}Li is light enough to keep under control the contribution of Final State Interactions (FSI) between the primary particles and the residual nucleus.

3.1 K^- absorption on two nucleons

Two techniques have been used so far to search for kaon bound states, namely the missing mass method, and the invariant mass spectroscopy. In the first case, the analysis is based on the study of $A(K^-, N)X$ inclusive or semi-inclusive spectra, where the presence of a peak in the momentum spectrum of the X recoiling particle could be interpreted as a bound state. In the second case, possible nuclear aggregates are deduced from the invariant mass spectra of the particles coming from their decay. The invariant mass approach is more complete and less subject to misinterpretation. The invariant mass of a particle pair may indicate the presence of a resonance, *i.e.* $(K^-pp) \to \Lambda p$ [10]. However, when such a resonant state is embedded in a nuclear medium, the invariant mass loses its original meaning [55]. The implications of such invariant mass of off-shell particles, called Quasi-Invariant Mass (QIM), are mainly two. The first one is that the invariant mass reconstructed from the decay of a bound state is not the mass of the bound state at all, but the QIM distributes broadly below the bound state energy. The second one is that the QIM is shifted and broadened by collisions with surrounding nucleons. Yamazaki and Akaishi in Ref. [56] suggested to the FINUDA Collaboration to study the QIM correlated to Dalitz Domains in order to explain the nature of bump measured by FINUDA among the possible interpretations. At the moment, the FINUDA statistics per target on the bump is not enough to fill completely the Dalitz Domains, which will be possible with a new 3 fb^{-1} data taking. With the present statistics in the bump it is possible to study the observables one at a time without correlating them.

The simplest way to get insight about an absorption process is to study the energy spectra and opening angles distribution of the particle pair detected in the final state. In light nuclei the processes in which two particles only are produced in an absorption reaction can be singled out by selecting events where

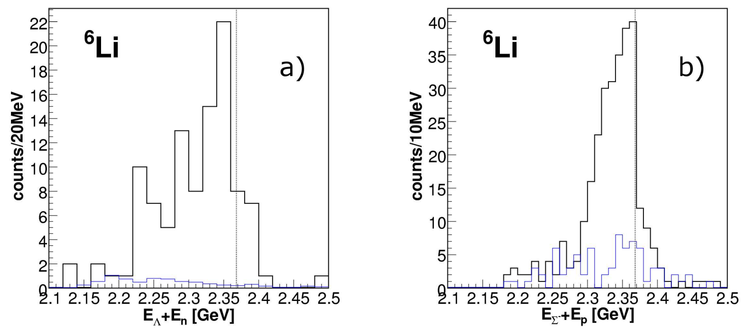

Figure 3.1: Total energy a) of the Λn final state and b) of the $\Sigma^- p$ final state in the K^{-6}Li reaction. The dashed vertical line shows the reaction Q-value. The blue histograms show the background contribution from fake neutrons. The spectra are not corrected for neutron efficiencies, that, however, decreasing for higher energies, would enhance the observed peak.

the sum of the energies of the emitted particles close up to the reaction Q-value [50]. This observation holds well for K^- absorption by "quasi"-deuterons, *i.e.*, (np) bound pairs inside the nucleus. On the other hand, the heavier the nucleus, the less reliable the selection (since FSI effects come into play).

Asking for a neutron in coincidence, few events (of the order of 50 per target) have been selected in the (Λn) final state [57]. The energy sum distribution for back-to-back particles, shown in Fig. 3.1a) for the K^{-6}Li case, is compatible with a peak close to the reaction threshold and this indicates the occurrence of a two-nucleon absorption. The same happens for exclusive events selected in the $(\Sigma^- p)$ channel, with the Σ^- fully reconstructed by its decay into π^- and n [57], as seen in Fig. 3.1b). As far as it is possible to infer from the small available statistics, no (or small [58]) effects from FSI is evident for ^{6}Li. This result confirms what was obtained in a semi-inclusive analysis of the proton momentum spectrum [12], where a clean signature of the $\Sigma^- p$ final state was seen for events on ^{6}Li targets – but not in ^{12}C, which was due to the overwhelming FSI effects in our inclusive event sample.

For (Λp) back-to-back selected events no peaks could be seen close to threshold, a fact that was already pointed out in Ref. [10] with the first data collected by FINUDA on light targets. Here a bump corresponding to a binding energy of 115 MeV was observed in the (Λp) invariant mass spectrum and was interpreted as a deeply-bound $(K^- pp)$ aggregate with a decay width of 67 MeV.

In the second FINUDA run, a good amount of (Λp) events (about $\times 8$ with respect to the first data taking) was collected on the two available ^{6}Li targets [14]. Also in this case the data were characterized by (1) the absence of a peak close to the reaction threshold and (2) the presence of a bump more than 100 MeV below this threshold, mainly composed by back-to-back events.

The possibility that this structure could simply come from the absorption of K^- on two nucleons in the $\Sigma^0 p$ final state, followed by Σ^0 electromagnetic decay, is still open and requires further investigation. Presently, the bump width and the relative Σ^0/Λ production strengths in K^- capture $((\Sigma(\text{no}\,\pi)/K^-_{stop} \div \Lambda(\text{no}\,\pi)/K^-_{stop}) \simeq 0.24$ [51]) does not seem to agree with this hypothesis. A kinematic fit tool could help to single out true $(\Sigma^0 p)$ events, which require 74 MeV/c slower Λ's. For this tool to work properly, a reasonable statistics is however necessary.

It is worth recalling that the E549 Experiment at KEK-PS followed the analysis of FINUDA in a study of ΛN final states in $K^-_{stop}{}^4$He [59]. Basically they observe a similar signal, but need further analysis to ascertain its nature, as their apparatus has a limited acceptance.

Then, concerning the study of K^- absorption on two nucleons, some more inputs are still welcome to fully understand our observations of the back-to-back (Λp) final state. In a new data taking of 3 fb^{-1} we'll be able to collect from the two foreseen Carbon targets a factor of 10 more statistics as compared to our first publication [10]; on ^{6}Li we could gather six times more statistics as compared to what was collected in 2006-2007 (roughly 400 events surviving the most selective cuts on track quality, length etc.) In general, with more statistics neutron coincidences will also be more easily studied, to tune our studies of the (Λn) and $(\Sigma^- p)$ final states.

3.2 K^- absorption on three and four nucleons

The absorption of a K^- on $3N$, $4N$ or on heavier nuclear fragments can be studied observing the correlations between Λ's and deuterons or tritons. On this respect, FINUDA has the lowest threshold on d's and is the only experiment able to observe t's.

3.2.1 (Λd) correlations

In the first FINUDA run, a total of 25 (Λd) events were collected out of the two available ^{6}Li targets [8]. A remarkable feature is the back-to-back correlation of $(\Lambda$-$d)$ pairs. The analysis of the few events available for the (Λd) channel seems to rule out the absorption of the K^- by three nucleons of ^{6}Li: the (Λd) invariant mass spectrum can only be reproduced if a gaussian signal is added to the contribution of $K^{-6}\text{Li} \to \Lambda d 3N$ reactions, namely, $[\Lambda d]nnp$, $[\Lambda d]nd$ and $[\Lambda d]t$, as shown in Fig. 3.2. These reactions are modeled by phase-space properly filtered through the apparatus acceptance. The fit delivers for the mass and width of the signal, produced at a rate of about $4 \times 10^{-4}/K^-_{stop}$, 3251 MeV/$c^2$ and $\sim$ 37 MeV, respectively.

The analysis of the missing energy distribution leads to interpret the $K^-_{stop}{}^6$Li reaction as due to $K^-_{stop}\alpha(d) \to \Lambda d n(d)$, in which the undetected neutron carries away the $\sim$ 25 MeV excess kinetic energy; the recoiling "quasi"-deuteron (d) inside ^{6}Li acts as a spectator. These results are confirmed by the data collected in the second run of FINUDA. As reported in Ref. [14], FINUDA can easily detect deuterons with momenta as low as 350 MeV/c by means of both the energy loss response from several detectors (OSIM, LMD's) and Time Of Flight measurements.

Later, the KEK-PS E549 Experiment [60] published an analogous analysis of (Λd) final states for K$^-$ stopped in ^{4}He. They are inclined to explain their observation, which confirms our experimental result, as simply due to a $3N$

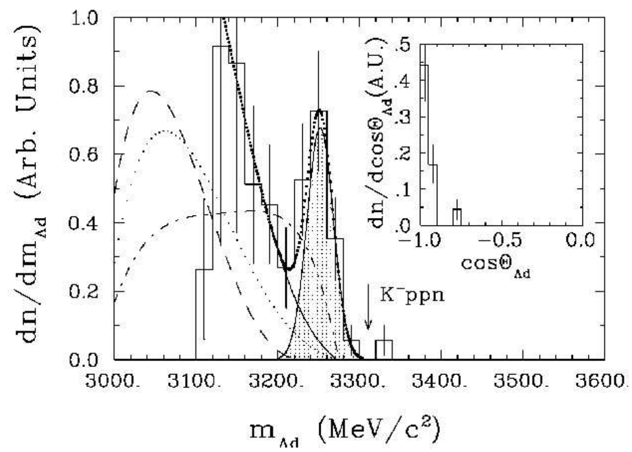

Figure 3.2: Invariant mass distribution of the (Λd) system for events from the ^{6}Li$(K^-_{stop},\ \Lambda d)3N$ reaction, solid line histogram; superimposed are the results of phase space simulations of several channels: dashed line $[\Lambda d]nnp$, dotted line $[\Lambda d]nd$, dot-dashed line $[\Lambda d]t$. The bold dotted-line is a fit of the experimental data with a Gaussian function and a linear combination of the above mentioned absorption reactions; the solid curve shows the contribution of the simulated background only.

absorption. However, as mentioned above, their acceptance correction (not applied in the paper) could be very sizeable and move the peak they observed to lower energies.

In the new data taking six times more statistics can be collected to study (Λd) correlations in K^- reactions on ^{6}Li. By cumulating the new data with the old ones, the statistics will start being enough to allow additional neutron coincidences to be studied. The measurement of a 25 MeV neutron in coincidence would be the strongest confirmation of the α capture mechanism in the Λdn.

The peak emerging so clearly in the (Λd) invariant mass spectrum for K^- absorption in ^{6}Li could not be seen in Carbon. The reason was most probably the strong effect of FSI's in a more complex system. The proposed data taking will help clarifying the absorption mechanisms even on Carbon since the available statistics will be a factor of ten larger than what we got in our first data taking. A sizeable statistics on ^{12}C and ^{28}Si, together with the already available statistics on ^{7}Li and ^{9}Be from the second data taking, will also allow us to give an A-dependence for the first time.

3.2.2 (Λt) correlations

To our knowledge, final (Λt) pairs following the K^- absorption reaction were studied only by an old bubble chamber experiment [53]. This experiment reports the branching ratio $(K^{-4}\text{He} \to \Lambda t)/(K^{-4}\text{He} \to \text{all}) = (3 \pm 2) \times 10^{-4}$ [53]. The analysis is based only on a kinematic fit, which was able to select three events out of about 3200. These three events however fitted equally well the alternative kinematic hypothesis Λdn. So, the production of tritons following the absorption at rest of K^-'s is still an untouched field.

(Λt) pairs were measured by FINUDA in the second run. These tritons were measured to have momenta larger than 600 MeV/c. Their mass identification was based on the dE/dx information deriving from OSIM and LMD's, which sets a threshold as low as 450 MeV/c.

Due to the high ionization (dE) of tritons, only forward particles could be reconstructed, as they cross a reduced amount of material before entering the tracker; backward tritons have to cross the full vertex/beam pipe region, and they most probably stop before being tracked.

By requiring $(\pi^- p)$ pairs in coincidence with t, about 40 events could be selected from all targets. Quite unpredictably, all the $(\pi^- p)$ pairs have an invariant mass which tightly closes the Λ value(see Fig. 3.3).

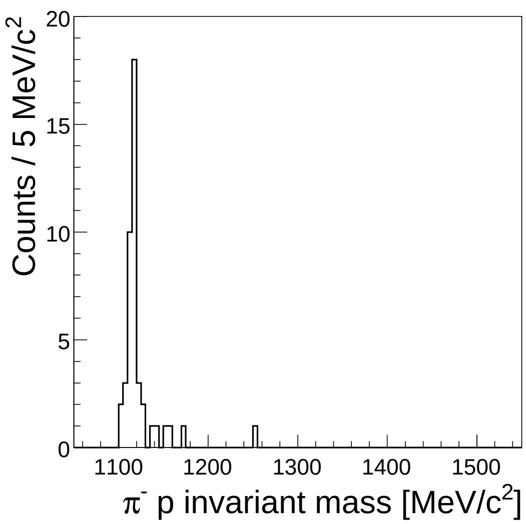

Figure 3.3: Invariant mass distribution of $\pi^- p$ pairs in coincidence with tritons, all targets, 2006-2007 FINUDA data.

The Λ momenta are large as well, exceeding $\sim$600 MeV/c. It is worth noting that Λ identification in FINUDA is possible in the whole apparatus acceptance. In all of these events the Λ and the t are back-to-back emitted, as shown in Fig. 3.4, open histogram. The events are few to allow a meaningful (Λt) invariant mass distribution to be obtained.

In Fig. 3.4 the shaded histogram shows the result of a phase-space simulation of the $K^-_{stop}\mathcal{A} \rightarrow \Lambda t N \mathcal{A}'$ reaction, where $\mathcal{A}$ stands for the nucleus on which the K^- interacts, and $\mathcal{A}'$ the residual bound nucleus. In the simulation the phase space reactions are performed on all our targets, and the results summed up properly weighted over the experimental number of K^- stopped in each target. The simple four-body phase-space is not able to explain the experimental back-to-back feature of the (Λt) pair (shaded histogram): the narrowness of the experimental $\cos\Theta_{\Lambda t}$ distribution indicates the occurrence of an exclusive

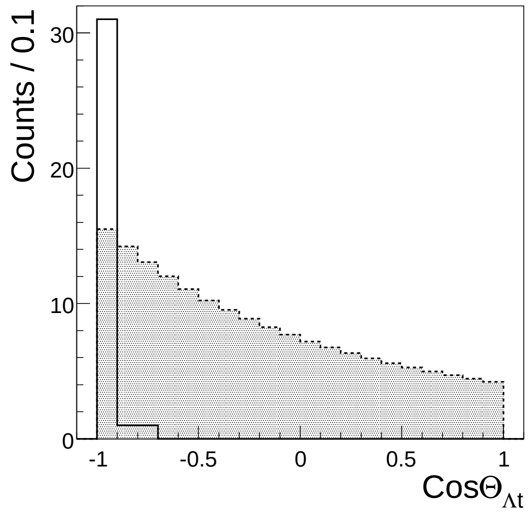

Figure 3.4: Opening angle distribution between Λ and t pairs, $\cos\Theta_{\Lambda t}$. Open histogram, experimental data; shaded histogram, phase-space simulation for the $K^-_{stop}\mathcal{A} \rightarrow \Lambda t N \mathcal{A}'$ reaction.

reaction process. In addition, the emission of (Λt) pairs occurs, as far as we can infer from our limited statistics, almost independently on the hit nucleus as if slightly affected by FSI effects.

Several kinematic hypotheses were tested by comparing the p_Λ vs p_t experimental distributions with the corresponding phase-space simulated ones, which were obtained applying similar kinematic cuts (opening angles, etc). Some results are shown in Fig. 3.5, 3.6 and 3.7. In Fig. 3.5 the momenta of t and Λ for the already mentioned $K^-_{stop}\mathcal{A} \rightarrow \Lambda t N \mathcal{A}'$ reaction is shown. The experimental data are superimposed to the scatter plot, and the phase space data are selected requiring $\cos\Theta_{\Lambda t} < -0.9$. The data points are spread over the high-intensity region of the reaction phase-space.

Fig. 3.6 shows the momenta of t and Λ for the direct $\Lambda t \mathcal{A}'$ production. The direct mechanism has a too small phase-space overlap to be able to explain just by itself the experimental distributions.

As well, the phase space distributions with pions in the final state, like in the $K^-\mathcal{A} \rightarrow \Lambda t \pi \mathcal{A}'$ shown in Fig. 3.7, completely miss the p_Λ vs p_t diffusion plot.

The few data collected agree better with the hypothesis of K^- absorption on many nucleons producing pionless final states with at least four bodies. However, the present statistics is poor to be able to infer on the reaction dynamics.

A new 3 fb^{-1} data taking will allow an almost six-fold statistics to be collected for ^{6}Li, offering moreover the chance to compare (Λt) production in ^{6}Li with that on a heavier nucleus like Carbon (10$\times$ more statistics than in 2003-2004), to test whether this final state stems from the K^- absorption on a

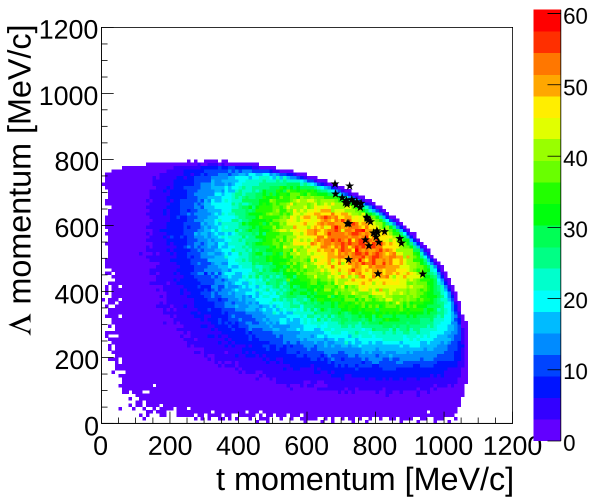

Figure 3.5: Scatter plot of p_Λ vs p_t for the four body reaction $K^-_{stop}\mathcal{A} \to \Lambda t N \mathcal{A}'$, where the notation $\mathcal{A}'$ represents a bound system of nucleons. The experimental data are represented by full stars.

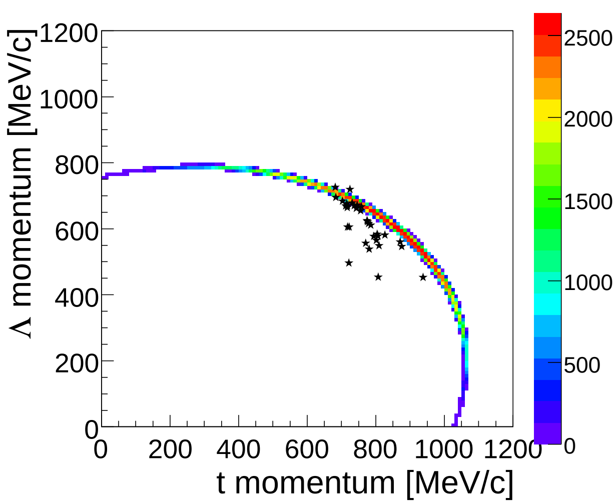

Figure 3.6: Scatter plot of p_Λ vs p_t for the direct reaction $K^-_{stop}\mathcal{A} \to \Lambda t \mathcal{A}'$, where the notation $\mathcal{A}'$ represents a bound system of nucleons. The experimental data are represented by full stars.

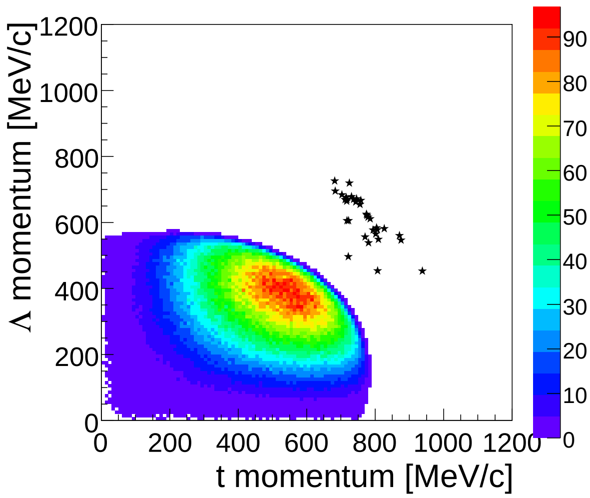

Figure 3.7: Scatter plots of p_Λ vs p_t for the multistep reaction in which an on-shell pion is produced in the final state, $K^-_{stop}\mathcal{A} \to \Lambda t \pi \mathcal{A}'$. The experimental data are represented by full stars.

"quasi"-α or on more complex nuclear systems.

Chapter 4

Interaction region and experimental installation

The mechanical compatibility of FINUDA with the configuration of upgraded DAΦNE has been checked and no relevant problems in this respect appear. Fig. 4.1, presented at the LNF Scientific Committee meeting of May 14, 2007, gives a pictorial view of FINUDA installed in the new DAΦNE configuration.

The installation of FINUDA in the new DAΦNE will proceed as in the previous first installation in which the beam-pipe had to be inserted. Moreover, we have to foresee the removal of the old beam-pipe still inserted in the spectrometer. So, regarding FINUDA, the installation will require 2.5 months, as in the 2003 installation, plus 5 days needed to remove the old beam pipe. This period includes also, according to the past experience, the alignment of FINUDA with respect to DAΦNE, and the magnet cooling with 7-10 days of cosmic rays data taking, without magnetic field, of the full FINUDA apparatus.

Before the FINUDA roll-in it is of course necessary to "swap" the configuration of IP1 and IP2 and moreover to install the four compensating superconducting solenoids in IP2. This huge job can be estimated to last four months, during which FINUDA can however perform in parallel all its own operations in the present parking position, and after the roll-in.

Of course, the central part of the new IP2 region with the central 500 μm Beryllium window (15 cm long and with a diameter of 6 cm), must be ready when the installation tasks begin.

Since the FINUDA installation can proceed in parallel with machine swapping, an overall total installation time for the third FINUDA roll-in of four and half months (including contingencies) seems reasonable.

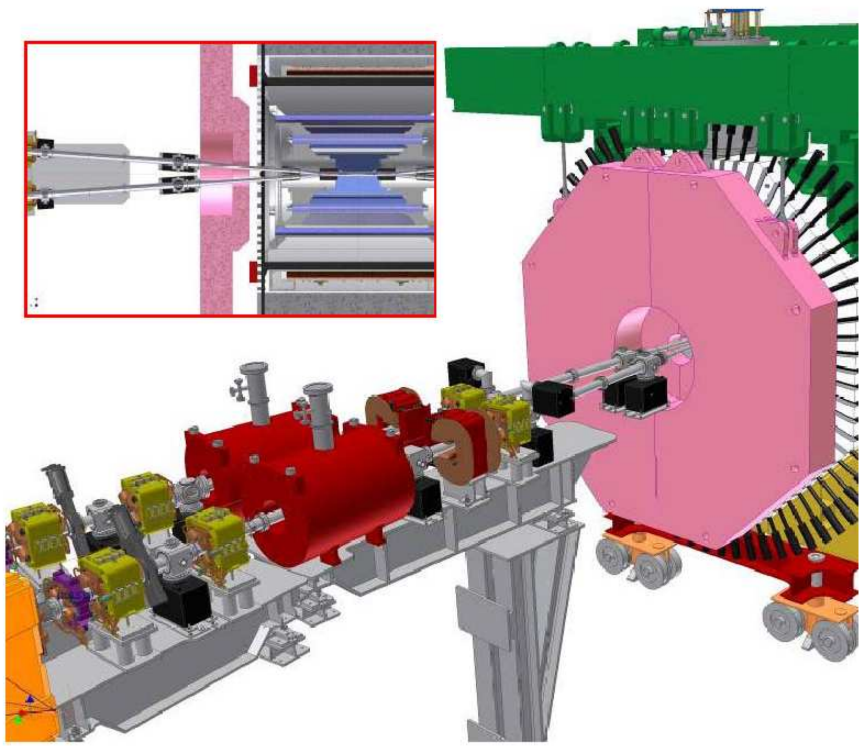

Figure 4.1: Pictorial view of FINUDA as installed on the upgraded setting of DAΦNE

Chapter 5

Data Acquisition System

The required FINUDA DAQ performances depend on the instantaneous luminosity provided by DAΦNE. During the 2003-2004 data taking the maximum instantaneous luminosity was $\mathcal{L} = 0.7\times10^{32}$ cm^{-2} s^{-1}, which corresponds to an hypernuclear type trigger rate of 8 Hz, while during the 2006-2007 data taking the maximum luminosity was $\mathcal{L} = 1.2\times10^{32}$ cm^{-2} s^{-1}, which gives 20 Hz hypernuclear type trigger rate. At the moment, two reliable scenarios can be imagined in order to foresee the maximum trigger rate for the next data taking: the former is a maximum instantaneous luminosity of 2.0×10^{32} cm^{-}2 s^{-1}, the latter 4.0×10^{32} cm^{-2} s^{-1}. Taking into account the machine background with the same level of signal over noise ratio as in the 2006-2007 data taking, the corresponding trigger rates are 40 and 80 Hz, respectively. To bear with these trigger rates the maximum dead time should be 2.5, 1.0 ms respectively, as shown in the Fig. 5.1.

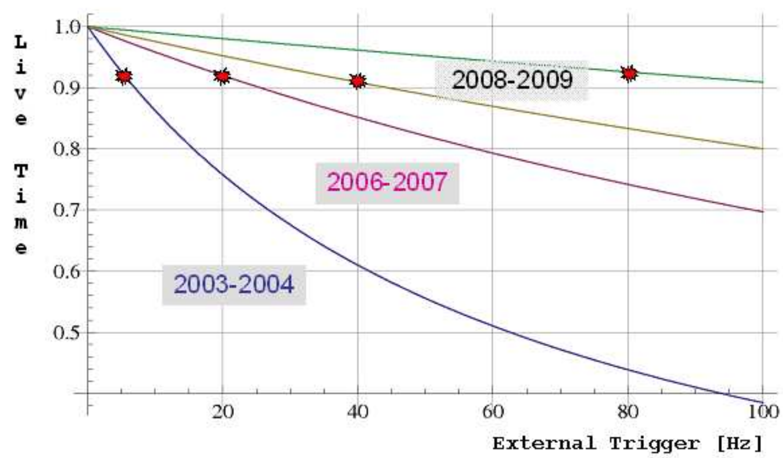

Figure 5.1: Live Time as function of External Trigger Rate for 2003-2004 Data Taking (blue), 2006-2007 Data-Taking (purple), 2.5 ms dead time (yellow) and 1.0 ms dead time (green).

Inside the FINUDA DAQ setup six independent readout branches can be identified: TOF, ISIM, OSIM, LMD, STB and the trigger system called GTS (General Trigger System). Fig. 5.2 shows the layout of the FINUDA readout system during the last data-taking. Each branch starts with the VME front-end electronics of FINUDA sub-detectors. The data are collected from VME to DAQ CPUs by means of VME-PCI Optical Link Bridges (CAEN V2718). The Table 5.1 shows the saturation rates reached for each branch during the last data taking.

Detector	Satur. Rate [Hz]	Dead Time [ms]	Sampl. Time [ms]	VME-PCI transfer [ms]
GTS	~ 530	~ 1.89		
GTS + TOF	~ 530	~ 1.89		
GTS + LMD	~ 530	~ 1.89		
GTS + STB	~ 455	~ 2.20		
GTS + ISI	~ 255	~ 3.92	~ 1.1	~ 2.1
GTS + OSI	~ 230	~ 4.35	~ 1.1	~ 2.4
All Together	~ 230	~ 4.35		

Table 5.1: Saturation rates reached of FINUDA DAQ branches during the 2006-2007 data taking. For ISI/OSI the sampling time and the VME-PCI transfer time are also reported.

It is clear that the slower branches are the Silicon Detector ones (ISI/OSI). Their maximum rate strictly depends on the bandwidth of the VME-PCI bridge link. A parallelization of the silicon readout system is feasible doubling the link between the VME crates and the PCI buses. This task consists in stretching two pairs of 70 m long LC-LC optical fibres between the DAΦNE Hall and the FINUDA Counting Room and in plugging two PCI cards in the DAQ CPU's, which collect the ISI/OSI data. The DAQ software is already compliant for this upgrade, which brings the time to collect the silicon data from 2.4 to 1.8 ms. A further improvement related to ISI/OSI readout is to reduce the sampling time of the Silicon Detector Channels. Bench tests have indicated the possibility to reduce this time from 1.1 ms to 0.6 ms, which brings the maximum dead-time of the silicon detectors to 0.6 ms + 1.8 ms = 2.4 ms, which fully comply the requirement to take data with a maximum instantaneous luminosity of 2.0×10^{32} cm^{-2} s^{-1}.

In order to further improve the DAQ a strong parallelization of TOF, LMD, STB and GTS readout is required. All these branches can be easily split into two different readout links, bringing their dead time to 0.9 ms. In this case, the optical fibres are few meters long and have to be stretched inside the FINUDA Counting Room, where both TOF, LMD, STB, GTS front-end electronics and DAQ CPU's are located. Besides, few slow CAMAC front-end electronic modules can be replaced by VME ones in order to make the data acquisition of GTS branch faster. The four fast branches can be used to make a decision with a 2^{nd} level trigger in order to discard the acquisition of the two slower detectors (ISI/OSI) by means of fast clear signal. The goal is to reduce the amount of data to be acquired, discarding the noisy and bad events which have a low

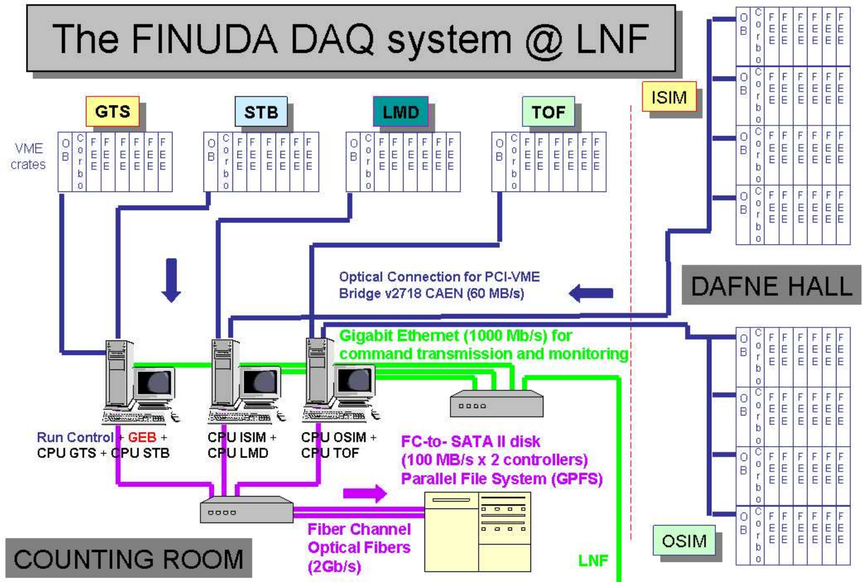

Figure 5.2: Layout of teh FINUDA readout system during the 2006-2007 Data Taking.

multiplicity in the faster branches (2 hits on LMD, 1 triplet in STB, 2 hits on TOF). Moreover, the present configuration of FINUDA DAQ permits a simple implementation of 3^{rd} level trigger which could be used to harden the previous selection. The LMD, STB and TOF data can be compared in order to decide if their hits give at least one rough track. Looking at 2006-2007 data sample it is possible to evaluate the combined effect of the two described selections as a 0.7 reduction factor. The hardware of 2^{nd} level trigger is already on the floor, indeed the fully programmable NIM outputs and inputs of v2718 controllers fit to this purpose. The software development for the 3^{rd} level trigger is in progress.

In this way for the FINUDA DAQ to acquire data with high efficiency becomes possible also with a maximum instantaneous luminosity of 4.0×10^{32} cm^{-2} s^{-1}. The I/O bandwidth required by the maximum luminosity is 20 KB/event $\times 80$ Hz $= 1600$ KB/s, which is bearable by the present disk system (FC-SATAII with GPFS > 100 MB/s). The required integrated luminosity of 3 fb^{-1} has to be related to 2006-2007 data-taking. 1 fb^{-1} of compressed raw data holds 5 TB, which means that 3 fb^{-1} could be saved in 15 TB, size that is compatible with an upgrade of the present I/O system.

The funds for the FINUDA DAQ upgrade have already been required and allocated by Com. Naz. III / INFN.

Chapter 6

Beam Time Request

With a foreseen increased luminosity of a factor of three with respect to the past, the necessary run time to collect 3 fb^{-1} will be similar to the previous data taking, which lasted approximately six months.

With an integrated luminosity of 3 fb^{-1}, FINUDA can significantly improve, about one order of magnitude in statistics, the data previously collected for ^{6}Li, ^{12}C and ^{28}Si. This last nucleus will be studied for the first time using stopped K^- with high statistics.

Acknowledgements

We are grateful to A. Gal, G. Garbarino, D.E. Lanskoy and T. Motoba for the useful discussions and suggestions that helped us to clarify the different physical topics addressed in this proposal.

Bibliography

[1] T. Bressani, in Proc. Workshop on Physics and Detectors for DAPHNE, Frascati, April 9-12 (1991), edited by G. Pancheri (Laboratori Nazionali di Frascati), 475-485;

[2] M. Agnello et al., LNF Internal Report, LNF-93/021 (IR) (1993);

[3] M. Agnello et al., LNF Internal Report, LNF-95/024 (IR) (1995);

[4] M. Agnello et al., Eur. Phys. J. A 33 (2007), 251;

[5] M. Agnello et al., Phys. Lett. B 622 (2005), 35;

[6] M. Agnello et al., Proc IX Int. Conf. on Hypernuclear and Strange Particle Physics, HYP 2006, Mainz, Oct.10-14, 2006, ed. J. Pochodzalla and Th. Walcher, SIF (Bologna), 57;

[7] M. Agnello et al., Phys. Lett. B 640 (2006), 145;

[8] M. Agnello et al., Phys. Lett. B 649 (2007), 25;
M. Agnello et al., Eur. Phys. J. A 33 (2007), 283

[9] Y. Akaishi and T. Yamazaki, Phys. Rev. C65 (2002), 044005;
Y. Akaishi and T. Yamazaki, Phys. Rev. C65 (2002), 044005;
A. Doté, Y. Akaishi and T. Yamazaki, Nucl. Phys. A738 (2004), 372;
Y. Akaishi, A. Doté and T. Yamazaki, Phys.Lett. B613 (2005), 140

[10] M. Agnello et al., Phys. Rev. Lett. 94 (2005), 212303;

[11] T. Nagae, Proc. IX Int. Conf. on Hypernuclear and Strange Particle Physics, HYP 2006, Mainz, Oct. 10-14, 2006, ed. J.Pochodzalla and Th. Walker, SIF (Bologna), 73;

[12] M. Agnello et al., Nucl. Phys. A 775 (2006), 35;

[13]) M. Agnello et al., Phys. Lett. B 654 (2007), 80;

[14] FINUDA Offline Group, Status Report on FINUDA Data Analysis, October 2007, document prepared for the LNF Scientific Committee

[15] M. Agnello et al. accepted for publication by Nucl. Phys. A

[16] W. Cheston and H. Primakoff, Phys. Rev. 92 (1953) 1537;

[17] J. J. Szymanski et al., Phys. Rev. C 43 (1991) 849;

[18] H. Noumi et al., Phys. Rev. C 52 (1995) 2936;

[19] O. Hashimoto et al., Phys. Rev. Lett. 88 (2002) 042503;

[20] J.H. Kim et al., Phys. Rev. C 68 (2003) 065201;

[21] S. Okada et al., Phys. Lett. B 597 (2004) 249;

[22] Y. Sato et al., Phys. Rev. C 71 (2005) 025203;

[23] B.H. Kang et al., Phys. Rev. Lett. 96 (2006) 062301;

[24] M.J. Kim et al., Phys. Lett. B 641 (2006) 28;

[25] A. Parreno and A. Ramos, Phys. Rev. C 65 (2002) 015204;

[26] K. Sasaki, T. Inoue and M. Oka, Nucl. Phys. A 669 (2000) 331; 678 (2000) 455;

[27] H. Outa, in Proc. of the International School of Physics "E. Fermi" Course CLVIII, edited by T. Bressani, A. Filippi and U. Wiedner (IOS Press, Amsterdam) (2004) 219;

[28] W.M. Alberico and G. Garbarino, Phys. Rep. 369 (2002) 1;

[29] E. Bauer, G. Garbarino, A. Parreno and A. Ramos, arXiv:nucl-th/0602066v1;

[30] accepted for publication by Nucl. Phys. A, NPA-D-08-00042R1;

[31] H. Tamura et al., Phys. Rev. Lett. 84 (2000) 5963;

[32] G. Garbarino, A. Parreno and A. Ramos, Phys. Rev. C 69 (2004) 054603;

[33] H. Bhang et al., Eur. Phys. J. A 33 (2007) 259;

[34] G. Garbarino, private communication.

[35] L. Majling and S. Gmuca, *Phys. At. Nucl.* 70 (2007) 1611.

[36] A.A. Korshenikov et al., *Phys. Rev. Lett.* 87 (2001) 092501.

[37] R.H. Dalitz, *Nucl. Phys.* A 754 (2005) 14c.

[38] Yu. B. Gurov et al., *Phys. At. Nucl.* 68 (2005) 491.

[39] D.E. Lanskoy, private comunication.

[40] L. Yuan et al., *Phys. Rev. C* 73 (2006) 044607.

[41] K.S. Myint and Y. Akaishi, *Prog. Theor. Phys. Suppl.* 146 (2002) 599.

[42] J. Schaffner-Bielich, Proc. of The IX International Conference on Hypernuclear and Strange Particle Physics, Springer-Verlag Berlin Heidelberg (2007) 387.

[43] S.V. Afanasiev et. al, Proc. of The IX International Conference on Hypernuclear and Strange Particle Physics, Springer-Verlag Berlin Heidelberg (2007) 165.

[44] T.R. Saito et. al, Proc. of The IX International Conference on Hypernuclear and Strange Particle Physics, Springer-Verlag Berlin Heidelberg (2007) 171.

[45] S. Ajimura et al., Production of Neutron-Rich Λ-Hypernuclei with the Double Charge-Exchange Reaction, Proposal for J-PARC 50 GeV Proton Synchrotron

[46] M. Agnello et al., *Phy. Lett.* B 640 (2005) 145.

[47] H. Hotchi, et al., Phys. Rev. C64, 044302 (2001).

[48] M. Iodice, et al., Phys. Rev. Lett. 99, 052501 (2007).

[49] T. Motoba, Nucl. Phys. A639 (1998) 135c.

[50] R. Bassalleck et al., Phys. Rev. C 19 (1979), 1893
P. Heusi et al., Nucl. Phys. A407 (1983), 429

[51] P. A. Katz, K. Bunnell, M. Derrick, T. Fields, L. G. Hyman and G. Keyes, Phys. Rev. D1 (1970), 1267

[52] C. Vander Velde-Wilcquet et al., Il Nuovo Cimento 39 (1977), 538

[53] M. Roosen, J.H. Wickens, Il Nuovo Cimento 66 (1981), 101

[54] T. Bressani et al., Nucl. Phys. B9 (1969), 427
J. Favier et al., Nucl. Phys. A169 (1971), 540
C. Cernigoi et al., Nucl. Phys. A352 (1981), 343
C. Cernigoi et al., Nucl. Phys. A456 (1986),

[55] T. Yamazaki and Y. Akaishi, Phys. Lett. B 453 (1999) 1.

[56] T. Yamazaki and Y. Akaishi, Nucl. Phys. A 792 (2007) 229 [arXiv:nucl-ex/0609041].

[57] H. Fujioka, PhD Thesis, University of Tokyo, 2008

[58] V. K. Magas, E. Oset, A. Ramos, H. Toki, Phys. Rev. C74 (2006), 025206

[59] T. Suzuki et al., arXiv:nucl-ex/0711.4943v1

[60] T. Suzuki et al., Phys. Rev C76 (2007), 068202